Int. J. Electrochem. Sci., 12 **(2017)** 517 – 528, doi: 10.20964/2017.01.46

International Journal of
ELECTROCHEMICAL
SCIENCE
www.electrochemsci.org

Effects of Pulsed-Electrodeposition Parameters on the Property of Aluminum Film onto Sintered NdFeB Magnets

Fang Xu[1], *Li Jiang*[1,2,*], *Jianhu Wu*[1], *Xiting Shen*[1], *Qiyun Huang*[1], *Yundan Yu*[1], *Chunan Cao*[2], *Guoying Wei*[1], *Hongliang Ge*[1]
[1]College of Materials Science and Engineering, China Jiliang University, Hangzhou, China;
[2]Department of Chemistry, Zhejiang University, Hangzhou 310027, China
[*]E-mail: jiangliwhu@126.com

Received: 17 October 2016 / *Accepted:* 22 November 2016 / *Published:* 12 December 2016

The aim of this study is to investigate the pulse-electrodeposition parameters on the property of aluminum (Al) film onto sintered neodymium-iron-boron (NdFeB) magnets at room temperature from acidic AlCl-1-ethyl-3-methylim-idazolium chloride ($AlCl_3$-EMIC) ionic liquid (2:1 molar ratio $AlCl_3$-EMIC). The effects of pulse frequency and duty ratio on the surface morphology, particle size, thickness, hardness, deposition rate, preferred orientation of Al grains and corrosion resistance of the Al films were researched. The results show that the increase of duty ratio can promote the deposition rate, particle size and relative surface roughness of Al films; while the increase of pulse frequency can accelerate the deposition rate of Al film and reduce its particle size and relative surface roughness. The optimum Al film with a smooth surface and good corrosion performance were obtained at the condition of i_p=12.5 mA/cm^2, r = 0.5, f = 5Hz.

Keywords: NdFeB magnets; Pulse-electrodeposition; Aluminum; Ionic liquid

1. INTRODUCTION

Sintered neodymium-iron-boron (NdFeB) magnets have a large application market for its excellent magnetic properties [1-3]. However, the applications are also hampered and limited by its poor corrosion resistance in actual working environment [4, 5]. Surface coating is usually used to enhance the anticorrosion property of sintered NdFeB magnets [6]. Especially, aluminum (Al) film is an ideal and environment-friendly surface protective material for sintered NdFeB magnets due to its good mechanical and physical properties, and small potential difference (0.06V) with the sintered NdFeB magnets in Na_2SO_4 solution (0.176 kmol·m^{-3})[7]. Till now, many works have been done on Al film's fabrication and corrosion resistance enhancements [8-10].

According to the literatures [11-13], brighter and flatter surfaces with tiny Al particles can be obtained at appropriate pulse parameters (pulse frequency and duty ratio) [14]. Researches of P. Giridhar et al [15] and A. Bakkar et al [16] indicated that the corrosion resistance of Al films increased with its reduced particle size (when the grain size decreases from micron range to 27nm, the corrosion current of Al film reduced to 1/10). The similar conclusion has also been confirmed by domestic scholars [8, 17]. However, the study on the Al film's fabrication with regulated crystal size on surface of sintered NdFeB magnets is fewer [18].

This work aims at pulsed-electrodepositing Al film onto sintered NdFeB magnets with finer particles and better corrosion resistance. The effects of the pulse frequency and duty ratio on the microstructure and corrosion resistance of Al film were also discussed in detail. It has great significance to explore the controllable preparation method and mechanism of Al film onto sintered NdFeB magnets, which can enrich Al electrodeposition theory within ionic liquid system, and further promote the industrial application of Al and /or Al-based coatings.

2. MATERIALS AND METHODS

2.1 Ionic liquid preparation

The ionic liquid consists of $AlCl_3$ (anhydrous powder, 99.99%, Aldrich) and EMIC (99%, Aldrich) with a molar ratio of 2:1. As ionic liquid should be prepared and stored in environment without oxygen and water vapor, in this research, the ionic liquid was prepared and stored in a glove box (DELLIX 5621101) filled with high-purify argon gas. After preparation, for further electrolyte purification, Al wires (≥99.99%) were immersed in it for 168 hours to remove residual water [19]. Finally, the EMIC- $AlCl_3$ ionic liquid became transparent with slightly yellow color [20].

2.2 Al film deposition

Laser was used to remove the native oxide layer of sintered NdFeB magnets before electrodeposition. After polished by $800^{\#}$ abrasive paper, the matrix was exposed to a 20 W laser beam (Nd: YAG of 1064 nm) for 5s within argon environment. Three-electrode system was adopted in the deposition process. Sintered NdFeB magnets (10.0 mm×10.0 mm×2.0 mm) served as working electrode. Al wire (diameter 2.0 mm, 99.99%, Aldrich) and Al sheet (20.0 mm×20.0 mm× 4.0 mm) were used as reference electrode and counter electrode, respectively. The deposition was conducted in the EMIC-$AlCl_3$ ionic liquid at room temperature by pulse-current polarization method controlled by electrochemical working station (CHI660E).

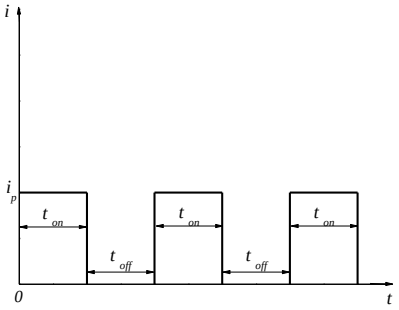

Figure 1. Schematic for square-pulse train for pulse-electrodeposition of Al film from the EMIC-$AlCl_3$ ionic liquid.

The used square-pulse current train in experiments is shown in Fig.1. The pulse-electrodeposition parameters employed in this work, pulse-current density (i_p, A·cm^{-2}), pulse frequency (f, Hz), on-current period (t_{on}, ms) and off-current period (t_{off}, ms), meet the relationship in Eqs.(1),

$$f = \frac{1}{t_{on}+t_{off}} \quad (1)$$

In order to distinguish the effects of pulse frequency and duty ratio on the microstructure and performance of Al films, the cathodic current for Al deposition was kept at 12.5mA·cm^{-2}, which has been preliminary researched[21]; while duty ratio (0.25, 0.5,0.75 and 0.8) and f (1, 2, 5, 8 and 10Hz) were varied in this experiment. For each Al film, the effective deposition time was 1 hour. After the pulsed-electrodeposition, the obtained Al films were washed by ethyl alcohol and acetone, then dried by nitrogen air. All experiments were operated in glove box filled with purified argon gas, where the moisture and oxygen content were maintained below 1.0 ppm.

2.3 Corrosion measurement

Electrochemical measurements (potentiodynamic polarization curves and electrochemical impedance spectroscopy) were used to investigate the corrosion of Al films. Experiments were performed on electrochemical working station (CHI660E) with the conventional three electrode cell in 3.5% NaCl aqueous solution. A platinum foil served as counter electrode and a saturated calomel electrode served as reference electrode. The measured potential in potentiodynamic polarization curves was $\pm$300mV vs. V_{ocp} (open circuit potential) with a scan rate of 0.5 mV·s^{-1}. In the measurement of electrochemical impedance spectroscopy (EIS), the frequency range between 100 kHz ~ 10 mHz with 5 mV perturbation signal was chosen. Duplicate experiment was performed at the same condition to make the experimental data more reliable.

2.4 Surface analysis

The structure and composition of Al films were analyzed by X-ray diffraction (XRD, Rigaku Ultima IV) and scanning electron microscopy (SEM, Philip XL-40FEG) coupled with an energy-dispersive X-ray spectrometer (EDS). Bench instrument (KLA-Tencor P6) was used to measure the

thickness of obtained Al films. Moreover, the hardness of specimen was determined with vickers microhardness instrument (HV-1000) at the applied load of 50g for 15s.

3. RESULTS AND DISCUSSION

As reported [22], in the electrodeposition process of Al film, the $AlCl_4^-$ ions is dominant in the electrolyte and reacts with the pure Al metal to produce $Al_2Cl_7^-$ ions, and then $Al_2Cl_7^-$ ions get electrons and revert to Al atom on matrix. The concentration and diffusion rate of $Al_2Cl_7^-$ ions in double electrode layer are the main factors affecting the Al electrodeposition process [23]. In the pulse-electrodeposition process, the pulse current density (i_p) during t_{on} period can promote the diffusion rate of $Al_2Cl_7^-$ ions and the initial nucleation of Al deposits on the surface; during t_{off} period, the recovery of $Al_2Cl_7^-$ ions concentration weakens the growth of the depletion layer and provide a better deposition condition for the next t_{on} duration. The successive plating cycles made the deposited Al films compact and smooth [24].

The composition of pulse-electrodeposited Al films were analyzed by EDS and shown in Fig.2. These deposited films consist of Al element and quite a small amount of O element, as tiny parts of film were oxidized by oxygen once it was exposed in the air. The Cl elements and C elements in the films may come from the traction and adsorption of ionic liquid during the deposition process [14].

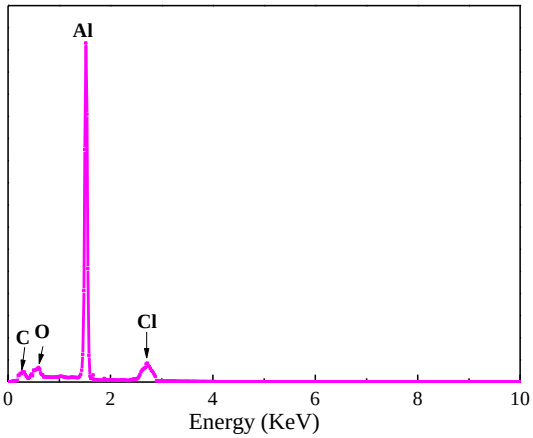

Figure 2. EDS patterns of Al films pulse-electrodeposited from EMIC-$AlCl_3$ ionic liquid

3.1 Effects of pulse frequency

Fig.3 shows the SEM images of Al films pulse-electrodeposited from EMIC-$AlCl_3$ ionic liquid at different pulse frequencies. The increase of pulse frequency reduces the diffusion time of ions to the cathode, and then the concentration polarization of cathode is promoted. As the pulse frequency increases from 1Hz to 10Hz, the particles of Al films are relatively refined.

Fig.4 shows the XRD patterns of Al film pulse-electrodeposited at different impulse frequencies. These films are constituted of pure *fcc* phase of Al metal [25] and exhibited [111]+[200] as the preferred orientation. The diffraction intensity of [200] is strengthened by lower the pulse frequency. It is known that peaks width can be used to determine the average grain size through the

Scherrer Equation [26]. The calculated data and other characters of Al films as the function of pulse frequency are shown in table 1. As the pulse frequency rises, the deposition rate and thickness of Al film both increase. The calculated Al particle size reduces relatively, which is the same regularity with that obtained from Fig.3.

The hardness of materials is relevant with its density, microstructure and component [27]. As the pulse frequency increase from 1 to 5 Hz, the hardness of Al films increases. It can be explained by the reduced plastic deformation of the matrix with Al grain refining and dispersive strengthening effects [28,29]. The maximum value of hardness (121Hv) is obtained when Al film deposited at pulse frequency of 5Hz. When pulse frequency increase from 5 to 10 Hz, the hardness of specimen declines. The reason is that the deposited smaller grains are conductive to coalescence during the t_{off} period and form irregular and larger aggregated particles (see Fig.1.), which reduces the hardness of films.

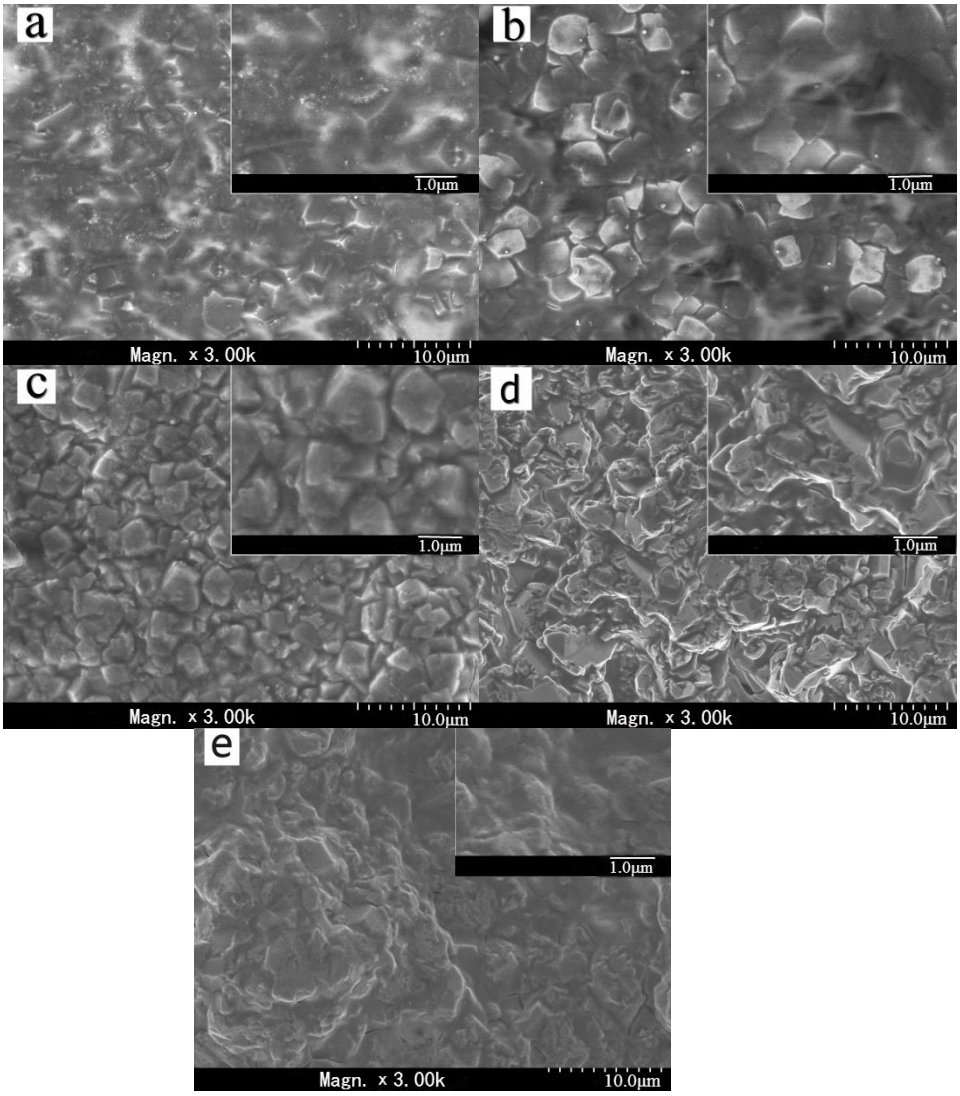

Figure 3. SEM images of Al films pulse-electrodeposited from EMIC-$AlCl_3$ ionic liquid at different pulse frequencies: i_p=12.5mA/cm^2, r=0.5, (a)1Hz; (b)2Hz; (c)5Hz; (d)8Hz; (e)10Hz

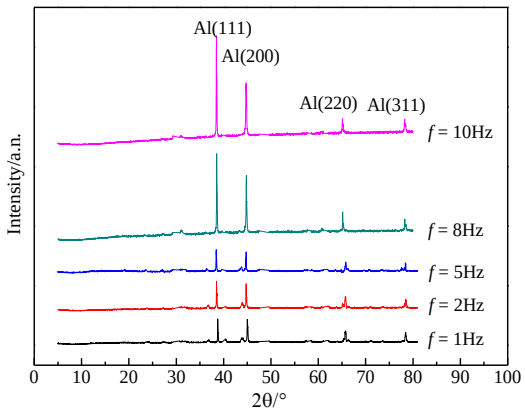

Figure 4. XRD patterns of Al films pulse-electrodeposited from EMIC-$AlCl_3$ ionic liquid at different pulse frequencies

Table 1. The characters of Al films pulse-electrodeposited from EMIC-$AlCl_3$ ionic liquid at different pulse frequencies

Frequency /Hz	1	2	5	8	10
Duty ratio(*r*)	0.50	0.50	0.50	0.50	0.50
Thickness/nm	880	900	910	940	960
Hardness/HV	62	81	121	95	76
Particle size/nm	84.256	82.130	81.997	80.680	76.579
Deposition rate/nm·s^{-1}	0.244	0.250	0.253	0.261	0.267

3.2 Effects of duty ratio

According to literatures [13,24], during t_{on} period, nucleation and growth of Al nanoparticles take place, leading to a drop in surface metal ions concentration and the emergence of progressively lower concentration gradients. And during t_{off} period, $Al_2Cl_7^-$ ion concentration on the surface of NdFeB magnet recovered and thus the side reactions are suppressed, resulting in a better deposition condition in the next t_{on} duration [11-13]. Fig.5 and Fig.6 show the SEM images and XRD patterns of Al films pulse-electrodeposited from EMIC-$AlCl_3$ ionic liquid at different duty ratios. As the duty ratio increases, the formations of Al films on the cathode surface are promoted and the Al particles on surface of films enlarge. The XRD patterns of Al films deposited at different duty ratios indicates that Al grains of films exhibit [111]+[200] as the preferred orientation. As the duty ratio decreases, the diffraction intensity of [200] improves, and the diffraction intensity of [311] weakens. The characters of Al film pulse-electrodeposited as the function of duty ratios are presented in table 2.

As the duty ratio increases from 0.25 to 0.8, the deposition rate of Al film increases from 0.231 to 0.269 nm/s; at the same deposition time, the thickness rises from 833nm to 970nm. The calculated grain size of Al film increases a little as the function of duty ratio, which is the same with the observation results from Fig.5. Moreover, the hardness of Al film increases first and then decreases with the increase of duty ratio. When duty ratio is 0.50, the hardness of Al film reaches to the maximum value.

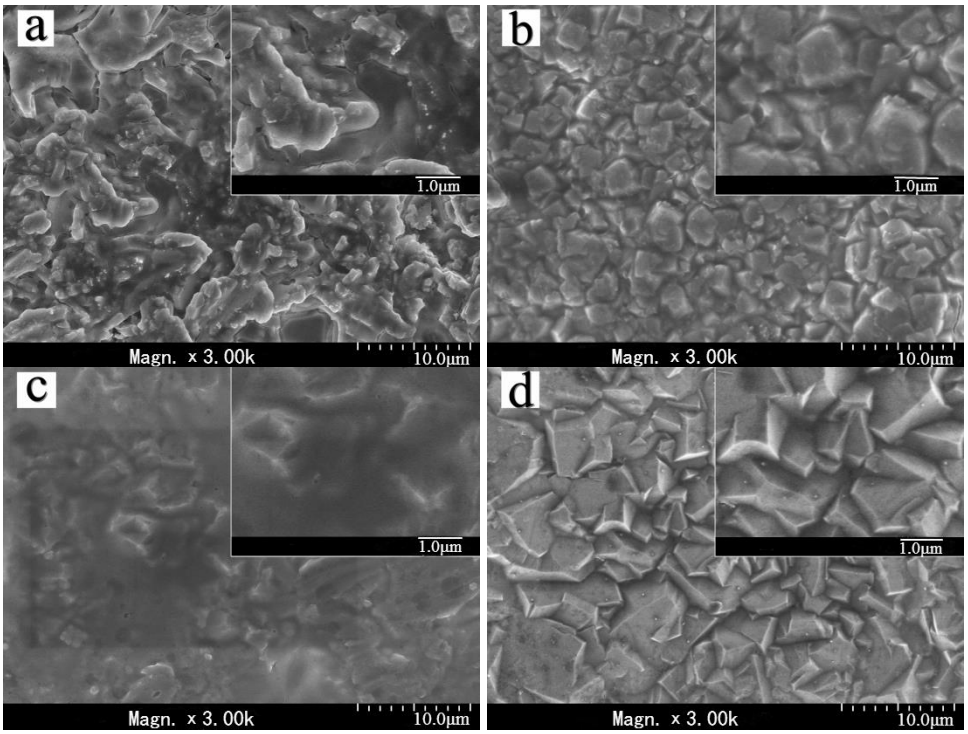

Figure 5. SEM images of Al films pulse-electrodeposited from EMIC-$AlCl_3$ ionic liquid of different duty ratios: i_p=12.5mA/cm^2, f=5Hz, (a)r=0.25, t_{on}=50ms, t_{off}=150ms; (b)r=0.5, t_{on}=100ms, t_{off}=100ms; (c)r=0.75, t_{on}=150ms, t_{off}=50ms; (d)r=0.8, t_{on}=160ms, t_{off}=40ms

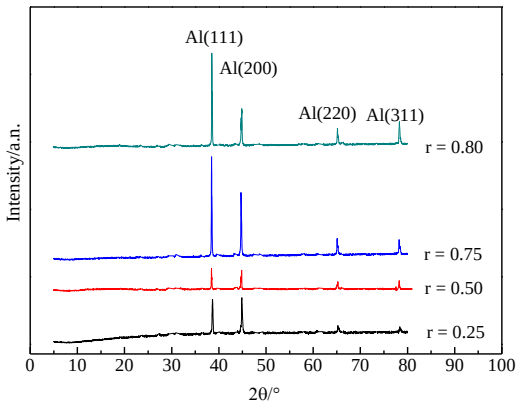

Figure 6. XRD patterns of Al films pulse-electrodeposited from EMIC-$AlCl_3$ ionic liquid at different duty ratios

Table 2. The characters of Al films pulse-electrodeposited from EMIC-$AlCl_3$ ionic liquid at different duty ratios

Duty ratio (r)	0.25	0.50	0.75	0.80
t_{on}(ms)	50	100	150	160
t_{off}(ms)	150	100	50	40
Frequency/Hz	5.0	5.0	5.0	5.0
Thickness/nm	833	910	920	970
Hardness/HV	86	121	99	90
Particle size/nm	80.976	81.997	85.433	90.446
Deposition rate/nm·s^{-1}	0.231	0.253	0.256	0.269

3.3 Corrosion performance

Figure 7 indicates the potentiodynamic polarization curves of Al films pulse-electrodeposited at different conditions. Its analyzed data are shown in table 3. Generally, the cathodic curves represent the reaction of hydrogen evolution, and the anodic curves are assumed to represent the Al film dissolution [30]. The relationship of corrosion rate (v) and corrosion current density (I_{corr}) is expressed as follows:

$$v = i / zFA = I_{corr} / zF \qquad (2)$$

where z is number of reaction electrons; F is faraday constant; A is electrode area. In the same reaction system, z and F are constants [31]. From the table 3, the Al film has the minimum corrosion current density of 6.303×10^{-5} A/cm^2 at the deposition condition of i_p=12.5 mA/cm^2, r=0.5 and f=5Hz.

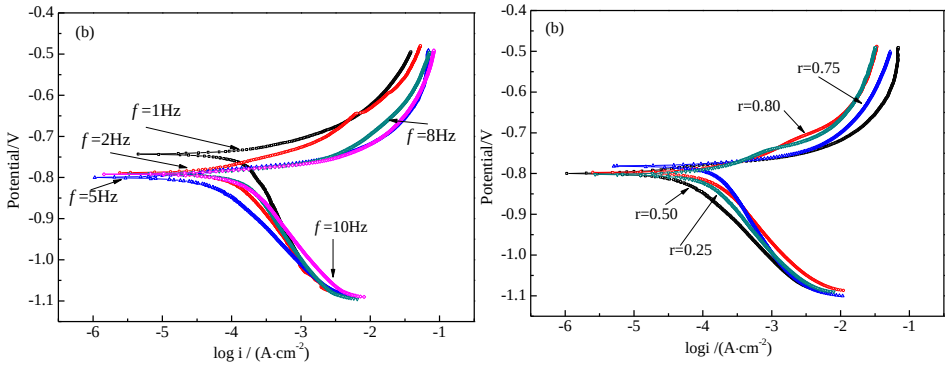

Figure 7. Potentiodynamic polarization curves of Al films pulse-electrodeposited at the different pulse frequencies (a) and duty ratios (b) immersed in 3.5%NaCl solution

Table 3. The analyzed electrochemical corrosion data related to potentiodynamic polarization curves

Sample	f/Hz	r	β_a /(mV·Decade^{-1})	β_c /(mV·Decade^{-1})	E_{corr}/V	I_{corr} /A·cm^{-2}
1#	1	0.50	8.965	3.553	-0.743	3.281×10^{-4}
2#	2	0.50	10.849	5.017	-0.789	2.302×10^{-4}
3#	5	0.50	10.910	6.594	-0.800	6.303×10^{-5}
4#	8	0.50	9.279	3.976	-0.791	1.450×10^{-4}
5#	10	0.50	9.758	4.729	-0.792	5.468×10^{-4}
6#	5	0.25	9.537	5.000	-0.797	3.799×10^{-4}
7#	5	0.75	9.898	3.764	-0.782	1.765×10^{-4}
8#	5	0.80	10.662	5.002	-0.802	2.453×10^{-4}

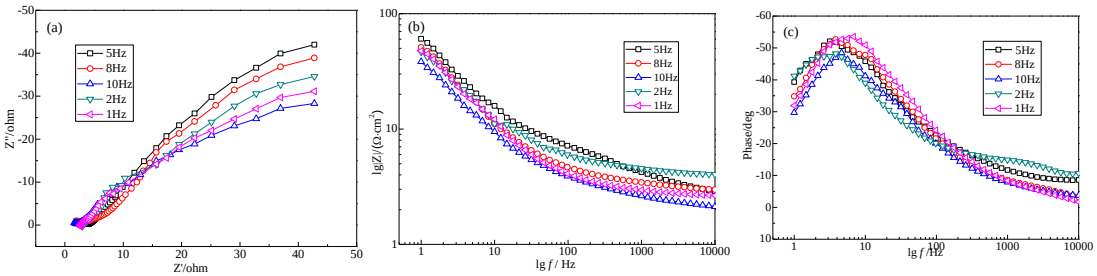

Figure 8. EIS plots of Al films pulse-electrodeposited from EMIC-$AlCl_3$ ionic liquid at different pulse frequencies

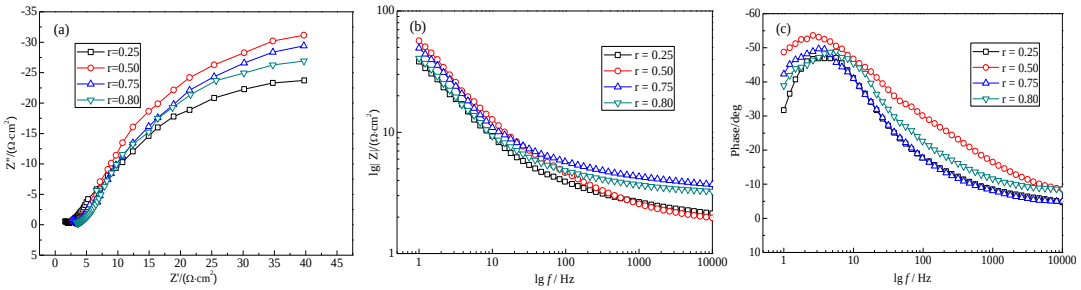

Figure 9. EIS plots of Al films pulse-electrodeposited from EMIC-$AlCl_3$ ionic liquid at different duty ratios

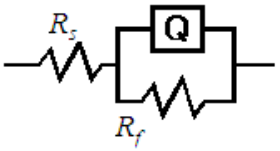

Figure 10. Equivalent circuit model of fitting EIS data

Table 4. EIS data for Al films pulse-electrodeposited from EMIC-$AlCl_3$ ionic liquid at different pulse frequencies and duty ratios

Sample	*f*/Hz	*r*	R_s/(Ω·cm^2)	CPE/(mF·cm^2)	n	R_f/(Ω·cm^2)	γ
1#	1	0.5	4.088	11.43	0.938	92.63	2.741
2#	2	0.5	2.581	11.07	0.942	113.2	2.655
3#	5	0.5	1.001	10.77	0.956	151.3	2.583
4#	8	0.5	3.113	9.78	0.953	123.4	2.345
5#	10	0.5	2.737	9.25	0.963	89.14	2.218
6#	5	0.25	2.332	9.81	0.938	81.93	2.353
7#	5	0.75	3.824	10.20	0.967	124.0	2.446
8#	5	0.8	1.846	11.66	0.972	101.3	2.796
Al foil	--	--	--	4.17	--	--	1.000

In traditional, EIS is always applied to describe the characters of corrosion process. The EIS plots of Al films pulse-electrodeposited from EMIC-$AlCl_3$ ionic liquid at different pulse frequencies and duty ratios show similar appearance as can be seen in Fig.8 and Fig. 9. In order to accurately simulate the EIS results, the equivalent circuit used for simulation of impedance response (shown in Fig.10) was composed of an electrolyte resistance (R_s), a charge transfer resistance (R_f), and a constant phase angle element (Q) [32]. The relative corrosion rate can be expressed using the reciprocal of this corrosion resistance ($1/R_f$) [33], shown in Fig.11. As the increase of pulse frequency, the corrosion of Al films in 3.5% NaCl solution decreases first and then increase. When Al film pulse-electrodeposited at pulse frequency of 5Hz, the relative corrosion rate is lower. Compared with the corrosion of films deposited at different duty ratios, when duty ratio is 0.5, the relative corrosion rate is lower. This regularity of relative corrosion rate ($1/R_f$) in Fig.11 is the same with that obtained from the analysis results of potentiodynamic polarization curves (shown in table 3).

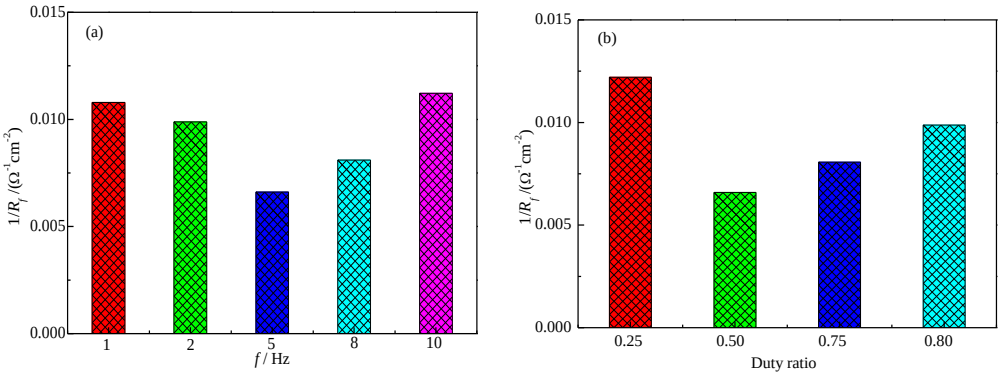

Figure 11. Changes of relative corrosion rate ($1/R_f$) calculated from EIS data

In addition, EIS has been also adopted to quantitatively evaluate the surface roughness of Al deposits. According to the references [11, 15], the surface of Al film will be oxided to form thin layer of alumina in the atmosphere. Provided that the thicknesses of the alumina and Al deposits are identical, the roughness factor of Al films can be evaluated from the capacitance value [11]. In this analysis process, the constant phase angle element *Q* can be analyzed by CPE and n. Since the value of n was 0.93~0.98 (shown in table 3), being close to 1, a CPE is considered to be a capacitor (C_f, CPE≈ C_f). C_f can be calculated from the following equation [16, 32]:

$$C_f = \frac{\varepsilon \varepsilon_f \gamma A}{d} \qquad (3)$$

Where ε is the permittivity of vacuum, ε_f is permittivity of film, γ is the roughness factor of the Al film, and A is the geometric surface area. The value of γ was assumed to be 1 for the flat Al foil. The total capacitance (C_T) can be given as follows:

$$\frac{1}{C_T} = \frac{1}{C_f} + \frac{1}{C_H} \qquad (4)$$

Where, C_H is capacitance of the Helmholtz layer. Since a typical value of C_H for most metals is in the range C_H≈10~100μF·cm^{-2}, it is extremely larger than C_f (a typical value of C_f is 3.6 μF·cm^{-2}), which can be neglected [11,33]. The value of γ is determined from the ratio of the capacitance of deposits to that on the flat Al foil as shown in table 3. The results indicate that as the increases of pulse frequency and decreases of duty ratio, the relative roughness (γ) of Al films declines. This change regularity is the same with that of Al particle size.

4. CONCLUSIONS

In this study, Al films were pulse-electrodeposited from EMIC-$AlCl_3$ ionic liquid onto sintered NdFeB magnets at room temperature. The effects of the pulse frequency and duty ratio on the microstructure and corrosion resistance of Al films onto sintered NdFeB magnets were also researched. In this study, EIS was adopted both to evaluated the corrosion resistance and the film's relative roughness, which has not been studied before. The deposition rate and thickness of Al films can be promoted as the increase of pulse frequency and duty ratio. However, the grain size and relative roughness of Al films reduced with the increases of pulse frequency and decrease of duty ratio. The

optimum Al film with a smooth surface and better corrosion performance were obtained at the conditions of i_p=12.5mA/cm^2, r=0.5, f=5Hz. Al grains of films exhibited [111]+[200] as the preferred orientation.

ACKNOWLEDGEMENTS
This research was supported by Zhejiang Provincial Natural Science Foundation of China (No. LY17B030006) and National Natural Science Foundation (No. 51401198, 51471156 & 51271168).

References

1. X. T. Li, M. Yue, W. Q. Liu, X. L. Li, X. F. Yi, X. L. Huang, D.T. Zhang, J. W. Chen, *J. Alloys Compd.*, 649(2015)656.
2. H. Sepehri-Amin, T. Ohkubo, M. Zaktonik, D. Prosperi, P. Afiuny, C.O. Tudor, K. Hono, *J. Alloys Compd.*, 694(2017)175.
3. H. Cha, K. Jeon, J. Yu, H. Kwon, Y. Kim, J. Lee, *J. Alloys Compd.*, 693(2017) 744.
4. X. Ding, L. Xue, X. Wang, K. Ding, S. Cui, Y. Sun, M. Li, *J. Magn. Magn. Mater.*, 416 (2016)247.
5. E. Isotahdon, E. Huttunen-Saarivirta, V. Kuokkala, *J. Alloys Compd.*, 692(2017) 190.
6. Y. Huang, H. Li, M. Zuo, L. Tao, W. Wang, J. Zhang, Q. Tang, P. Bai, *J. Magn. Magn. Mater.*, 409(2016)39.
7. H. Sepehri-Amin, T. Ohkubo, T. Shima, *Acta Mater.*, 60(2012)819.
8. L. Y .Wei, Master's degree thesis of Harbin Engineering University, 2009,01.
9. J. Chen, G. P. Ling. *Mater. Prot.*, 44(2011)11.
10. S.D. Mao, H. X. Yang,Z. L. Song, *Corros. Sci.*, 53(2011)1887.
11. J. Tang, K. Azumi, *Electrochim. Acta*,56 (2011) 1130.
12. H. Yang, E. O. Fey, B. D. Trimm, N. Dimitrov, M. S. Whittingham,*J. Power Sources*, 272 (2014) 900.
13. B. Li, C. Fan, Y. Chen, J. Lou, L. Yan, *Electrochim. Acta*, 56 (2011) 5478.
14. F. Liu, Y. Deng, X. Han, W. Hu, C. Zhong, *J. Alloys Compd.*, 654 (2016) 163.
15. P.Giridhar, S.Z.E. Abedin, F. Endres, *Electrochim.Acta*, 70(2012)210.
16. A. Bakkar, V. Neubert, *Electrochim. Acta*,103(2013)211.
17. D. H. Yang, Master's degree thesis of Chongqing Institute of Technology,2008,05.
18. E. Chen, K. Peng, W. Yang, J. Zhu, D. Li, L. Zhou, *Trans. Nonferrous Met. Soc. China*, 24(2014)2864.
19. J. Vaughan, D. Dreisinger, *J. Electrochem. Soc.*, 155(2008)D68.
20. W. Zhang, G. P. Ling, *Surf. Eng.*, 42(2013)66.
21. L. Jiang, Z. Jin, F. Xu, Y. Yu, G. Wei, H. Ge, Z. Zhang, C. Cao, *Surf. Eng.*, 32(2016)18.
22. D. Xue, Y. Chen, G. Ling, K. Liu, C. Chen, G. Zhang, *Fusion Eng. Des.*, 101(2015)128.
23. W. Zhang, G. P. Ling, *Surf. Tech.*,42(2013)66.
24. S.A. Lajevardi, T. Shahrabi, *Appl. Surf. Sci.*, 256 (2010) 6775.
25. D. Pradhan, R. G. Reddy, *Mater. Chem. Phys.*, 143(2014)564.
26. M.T. Tanvir, Y. Aoki, H. Habazaki, *Thin Solid Films*, 517 (2009) 6711.
27. U. Bardi, S. Caporali, M. Craig, A. Giorgetti, *Surf. Coat. Tech.*, 203(2009)1373.
28. T. Q. Mei, G. N. Yu, L. M. He, Y. R. Pei. *J. Chin. Soc. Corros. Prot.* 31(2011)319.
29. Y. Li, PhD thesis, Kuming University of Science and Technology, Kunming, China, 2011, 23-56.
30. Y.W.Song, E.H. Han, D.Y. Shan, C.D. Yim, B.S. You, *Corros. Sci.*, 60(2012) 238.

31. Y. W. Song, D. Shan, R. Chen, F. Zhang, E.H. Han, *Mater. Sci. Eng. C.*, 29(2009) 1039.
32. J. Q. Zhang, Electrochemical Measurement Technology. Chemical Industry Press, 2010.
33. C. N. Cao, J. Q. Zhang, Introduction of electrochemical impedance spectroscopy, Science press, 2002.